Available online at www.sciencedirect.com
ScienceDirect
Journal of Nuclear Materials 376 (2008) 265–268
journal of nuclear materials
www.elsevier.com/locate/jnucmat

Spectroscopic and microscopic investigation of the corrosion of D-9 stainless steel by lead–bismuth eutectic (LBE) at elevated temperatures. Initiation of thick oxide formation

Allen L. Johnson [a,c,*], Dan Koury [b], Jenny Welch [b], Thao Ho [a], Stacy Sidle [c,1], Chris Harland [c,1], Brian Hosterman [b], Umar Younas [b], Longzhou Ma [c], John W. Farley [b]

[a] Department of Chemistry, University of Nevada, Las Vegas (UNLV), 4505 S. Maryland Parkway, Campus Box 4003, Las Vegas, NV 89154-4003, USA
[b] Department of Physics, UNLV, 4505 S. Maryland Parkway, Campus Box 4002, Las Vegas, NV 89154-4002, USA
[c] Harry Reid Center, University of Nevada, Las Vegas, 4505 S. Maryland Parkway, Campus Box 4009, Las Vegas, NV 89154-4009, USA

Abstract

Corrosion of 316/316L stainless steel by lead–bismuth eutectic (LBE) at elevated temperature was investigated by examination of samples after 1000, 2000, and 3000 h of exposure at 550 °C, using SEM, XPS with sputter depth profiling, and TEM. The process by which localized oxide failure becomes extensive thick oxide formation was investigated. Under our experimental conditions, iron was observed to migrate outward while chromium did not migrate above the original metal surface. The thin oxide layer on the D-9 sample resembled 316L cold-rolled samples, while the thick oxide on D-9 resembled annealed 316L oxide. With continued exposure, thick oxide grew to cover the entire surface.

1. Introduction

Lead–bismuth eutectic (LBE) is of interest as a coolant in the design of fast reactors and also as both a coolant and a spallation target in proposed transmutation schemes for radioactive waste. Unfortunately, hot LBE corrodes many engineering materials. Studies of corrosion in the LBE/stainless steel system are important in assessing the feasibility of transmutation of nuclear waste.

In previous work by our group [1], the importance of surface preparation in the corrosion of 316 stainless steel by LBE was investigated. Two samples with the same composition but different surface preparations were studied: a cold-rolled sample was compared with an annealed sample. The cold-rolled sample had an order of magnitude less corrosion than the annealed sample. The cold-rolled sample had a thin (~1 μm) oxide layer, primarily of chromium oxide, while the annealed sample had a complex oxide structure (a layer of iron oxide over a mixture of chromium and iron oxide) tens of microns thick.

2. Experimental

Samples of 316/316L class nuclear grade stainless steel (cold-rolled, annealed or D-9) were exposed in the oxygen-controlled (0.03–0.05 wppm oxygen) LBE loop at the Institute for Physics and Power Engineering (IPPE) in Obninsk, Russia, under contract with Los Alamos National Laboratory [2]. The IPPE samples were exposed to oxygen-controlled LBE for 1000, 2000, and 3000 h at temperatures of 550 °C and flow rate of 1.9 m/s. A total of four samples from IPPE were examined using SEM, XPS with sputter depth profiling, and TEM.

* Corresponding author. Address: Department of Chemistry, University of Nevada, Las Vegas (UNLV), 4505 S. Maryland Parkway, Campus Box 4003, Las Vegas, NV 89154-4003, USA. Tel.: +1 702 895 0881; fax: +1 702 895 4072.
E-mail address: allen.johnson@unlv.edu (A.L. Johnson).
[1] Summer 2003 Undergraduate Research Student at UNLV.

0022-3115/$ - see front matter © 2008 Elsevier B.V. All rights reserved.
doi:10.1016/j.jnucmat.2008.02.005

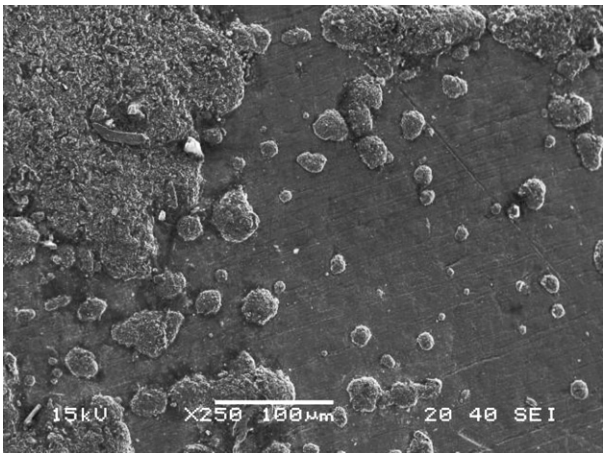

Fig. 1. SEM image of surface of D-9 sample after 2000 h. of exposure to LBE at 550 °C. Note patchy thick oxide covering part of the surface.

3. Results

D-9 is a standard nuclear grade steel, with a typical composition 68Fe, 13.6Cr, 0.85 Si, 13.6Ni, 0.04C, 1.11 Mo, 2.1Mn, and 0.3 Ti, and a proprietary surface treatment by Carpenter Technologies. A D-9 sample was exposed to LBE at 550 °C, and then examined by SEM (Figs. 1–3). After 2000 h of exposure, the surface is partially covered by small patches of thick oxide, as shown in Fig. 1. After 3000 h of exposure, the patches of oxide have grown to cover nearly the entire surface.

D-9 was examined in transverse section by SEM using backscattered electrons. The result is shown in Fig. 2, with the bulk metal at the bottom, epoxy (black in the image) at the top, and the thick oxide layer in between. The outer oxide layer is outside the original boundary of the steel and is an iron oxide. The inner layer of oxide is depleted in iron and is an iron/chromium oxide. Thus, iron has

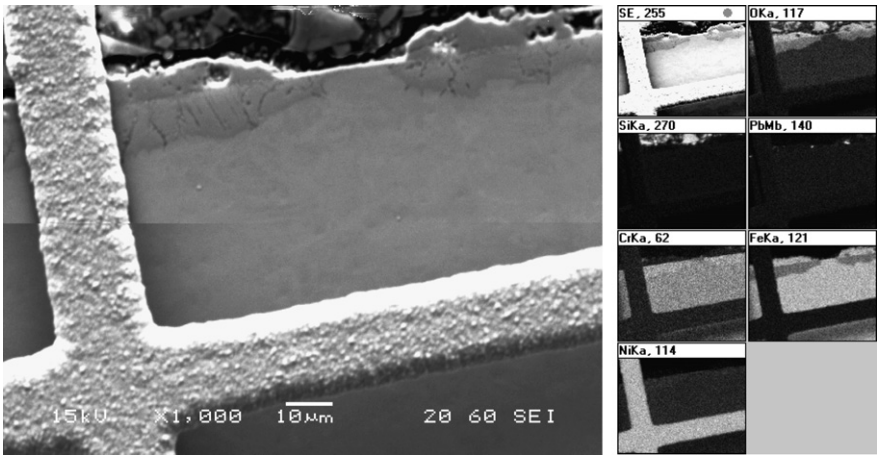

Fig. 2. Patchy oxide on D-9. Note that the inner FeCr oxide is below the original metal surface whereas the outer Fe oxide is above the original metal surface. Small lead inclusions can be seen below the outer oxide where the backscattered image shows oxide imperfections.

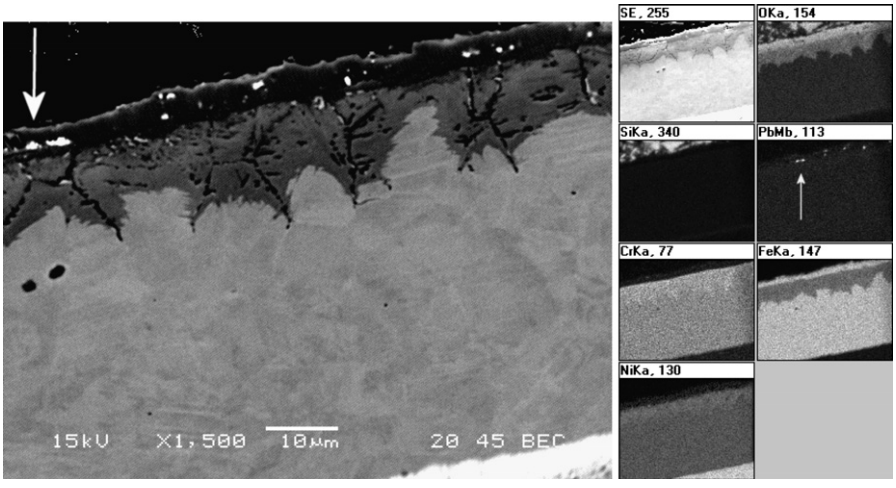

Fig. 3. Backscattered electron image of transverse section of D-9 steel sample, showing thick oxide morphology. Note diffusion channels in the inner oxide and correlation between diffusion channels and metal grains. Arrows show lead inclusions.

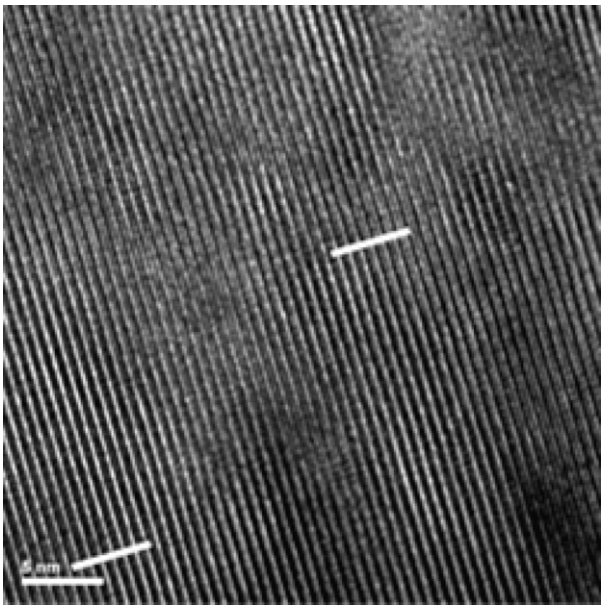

Fig. 4. TEM image of thin oxide in 316L cold-rolled sample, showing crystalline structure.

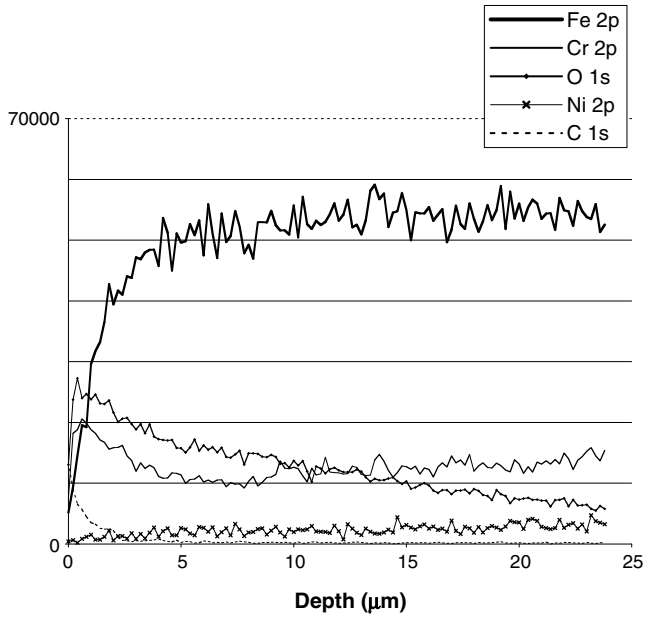

Fig. 5. Sputter depth profile of a D-9 sample exposed to LBE for 1000 h. at 550 °C. The portion of the surface investigated was not covered with visible oxide (i.e. was thin oxide).

moved outward to form the outer oxide layer, while oxygen has moved inward to form the inner oxide layer. The backscattered image suggests that the corrosion of the inner oxide may undercut the thin initial oxide. Chromium does not significantly migrate outside the steel surface in these experiments. The migher magnification backscattered SEM image of Fig. 3 shows the inner oxide layer has an intriguing pattern of channels of diffusion/attack, sometimes along grain boundaries.

At grain boundaries oxygen and chromium are observed to increase with exposure, while nickel and iron decrease. Silicon and manganese also increase at grain boundaries. Minor lead inclusions appear typically under oxide that has been compromised.

The mechanism of oxidation has been recently been modeled extensively (using a one-dimensional model) by Steiner et al. [3] who find that oxygen transport in LBE is of critical importance. Zhang and Li [4] provide a recent review of the experimental and theoretical literature, and the consensus oxidation phenomena agree with our observations. One-dimensional descriptions dominate the literature.

Fig. 4 shows a striking regular crystalline pattern of the thin oxide observed using TEM. The spacing can be measured (0.7 nm) from this image. The thin oxide is much more crystalline than the thick oxide. The outer oxide does not show evident layer spacing in TEM and appears in SEM to be composed of very small grains.

Tests were performed on a sample of D-9 that was exposed to LBE for 1000 h at 550 °C. An area of the surface that was not covered by the visible oxide was studied by XPS sputter depth profiling. The results are shown in Fig. 5. The data are consistent with the presence of either chromia (Cr_2O_3) or an iron/chromium spinel. These data are similar to what our group observed [1] in the cold-rolled 316L samples.

4. Discussion

The observation of preferential corrosion at localized sites indicates that thick oxide forms at failure regions of the thin oxide. We observe the formation of spinel undercutting the thin oxide without the formation of an iron cap layer. This observation suggests that iron does not migrate through the thin oxide except at localized failure regions. Hence the thick oxide is not as resistant to materials transport during corrosion as the original thin oxide. Other work in this symposium [5–7] report similar results. Our work suggests that a one dimensional picture of oxide formation in LBE corrosion of steel is inadequate to describe the conversion from the thin oxide to the thick oxide.

Acknowledgements

We wish to acknowledge FEI, Inc. for preparing TEM sample preparation. A portion of the research was performed at the Environmental Molecular Sciences Laboratory, Richland, WA, USA. Major funding is gratefully acknowledged from the Transmutation Research Program of the Harry Reid Center for Environmental Studies, DOE Office of Nuclear Energy, Science and Technology, under the Advanced Fuel Cycle Initiative Contracts DE-FG04-2001AL67358 and DE-AC03-76SF00098. Stacy Sidle, Chris Harland, and Jenny Welch, were supported by NSF REU grant # PHY-0139584 during 2003 (Sidle and Harland) and 2005 (Welch).

References

[1] A.L. Johnson, D. Parsons, J. Manzerova, D.L. Perry, D. Koury, B. Hosterman, J.W. Farley, J. Nucl. Mater. 328 (2004) 88.
[2] J. Zhang, N. Li, Y. Chen, A.E. Rusanov, J. Nucl. Mater. 336 (2005) 1.
[3] H. Steiner, C. Schroer, Z. Voß, O. Wedemeyer, J. Konys, J. Nucl. Mater. 374 (2008) 211.
[4] J. Zhang, N. Li, J. Nucl. Mater. 373 (2008) 351.
[5] P. Hosemann, H.T. Thau, A.L. Johnson, S.A. Maloy, N. Li, J. Nucl. Mater. 373 (2008) 246.
[6] P. Hosemann et al., J. Nucl. Mater. 376 (2008) 289.
[7] L. Martinelli et al., J. Nucl. Mater. 376 (2008) 282.